Robust control of entanglement in a nitrogen-vacancy center coupled to a ^{13}C nuclear spin in diamond

R. S. Said and J. Twamley
Centre for Quantum Computer Technology, Department of Physics & Electronic Engineering, Faculty of Science, Macquarie University, Sydney, New South Wales 2109, Australia
(Received 24 March 2009; published 1 September 2009)

We address the problem of generating a robust entangling gate between electronic and nuclear spins in a system of a single nitrogen-vacancy center coupled to a nearest ^{13}C atom in diamond against certain types of systematic errors such as pulse-length and off-resonance errors. We analyze the robustness of various control schemes: sequential pulses, composite pulses and numerically optimized pulses. We find that numerically optimized pulses, produced by the modified gradient ascent pulse engineering (GRAPE) algorithm, are more robust than the composite pulses and the sequential pulses. The optimized pulses can also be implemented in a faster time than the composite pulses.

DOI: 10.1103/PhysRevA.80.032303 PACS number(s): 03.67.Bg, 03.65.Ud, 42.50.Dv, 14.70.Bh

I. INTRODUCTION

Solid-state technologies hold great promise toward the fabrication of large scale quantum devices. Hence, theoretical and experimental investigations into the control of quantum information in such systems have progressed quite rapidly and candidate technologies include phosphorus donor electrons in silicon nanostructures [1,2], Gallium Arsenide quantum dots [3], superconducting Cooper-pair boxes [4], circuit quantum electrodynamics [5], and nitrogen-vacancy (N-*V*) centers in diamond [6]. A system based on N-*V* centers in diamond is attractive because, at room temperature, the N-*V* center displays strong spin polarization under optical pumping, exhibits remarkable photostability and shows high fluorescence quantum yield [7]. The electronic spins of the N-*V* center are initialized and measured by optical means and can be manipulated via irradiation by microwave (MW) radiation. Through a hyperfine coupling, an interaction between the electronic spins of the N-*V* center and the nuclear spin of a nearby ^{13}C atom can be exploited to encode two quantum bit of information, and quantum logic can be executed via the application of microwave and radio-frequency (RF) radiation. Observations of Rabi oscillations of the electronic spin [8], and the nearby nuclear spin [9] in the N-*V* center, performed by optically detected magnetic-resonance (ODMR) techniques, have paved the way for a realization of the N-*V* center based quantum computer [10]. A more advanced quantum information processing (QIP) task that is a demonstration of three-qubit entanglement has been recently reported in the literature [11]. This latest development points to possibilities of multiqubit QIP implementations. However, the use of accidental nearby nuclear spins poses some difficulties toward the scaling up this technology.

Because the qubit system interacts with an environment, QIP is subject to unavoidable errors. Hence, error control and error avoidance schemes are necessary to achieve reliable quantum computation. The errors can occur either in a random or a systematic fashion. The random errors are due to decoherence processes, while systematic errors occur when the physical apparatuses controlling the dynamics of the system operate in an imprecise but reproducible manner. In the spin system driven by microwave or radio-frequency radiation, nonideal values of the radiation properties (i.e., amplitude, phase, duration, and frequency) cause such systematic errors. A common type of systematic error, namely, *pulse-length error* (PLE), occurs when the radiation (assumed to be a rectangular pulse) is resonant with the target spin transition but whose application time or amplitude differs in an unknown (but fixed in time) quantity from the ideal value. Another type of systematic error is *off-resonance error* (ORE). Off-resonance errors arises when the frequency of the control radiation is unexpectedly not on resonance with the spin transition and spin dynamics proceeds with an unknown (but unchanging) detuning parameter.

In this paper, we describe schemes for the generation of an entangling gate between the electronic and nuclear spins in the N-*V* center in diamond, which are robust against PLE and ORE systematic errors. We investigate effects of such errors in a sequential application of rectangular pulses of microwave and radio frequency. Furthermore, we compare the fidelity of such pulses with their more robust counterparts: composite pulses and numerically optimized pulses produced from a modified algorithm of gradient ascent pulse engineering (GRAPE) [12]. The sequential pulses have previously been used to generate two-qubit entanglement [7], while composite pulses are known to be capable of correcting systematic errors in nuclear-magnetic-resonance (NMR) experiments [13]. In the next section, we describe the N-*V* system and introduce the sequential pulses required to create a particular entangled state in this system. Section III examines the decrease in gate fidelity due to systematic errors when we adopt various methods of implementing this gate: using sequential pulses, using robust composite pulses and using robust GRAPE pulses. Results of the numerical simulations and performance comparisons between the composite and GRAPE pulses against PLE and ORE systematic errors are discussed in Sec. IV. The last section is conclusion and some remarks on possible extensions of our work. Overall we find that GRAPE pulses are more robust than the sequential and composite pulses, and faster to implement than the composite pulses.

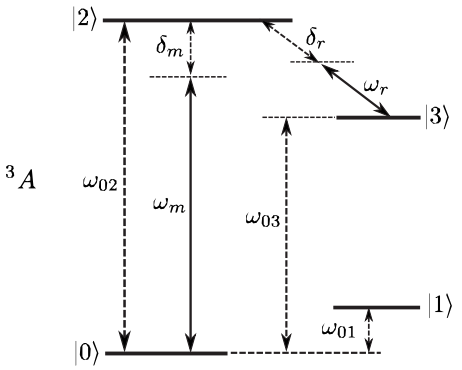

FIG. 1. Energy level diagram of the ground state ^{3}A of the N-V center in the absence of an external magnetic field. The $|0\rangle-|1\rangle$ and $|2\rangle-|3\rangle$ energy splittings are due to the hyperfine interaction between the N-V electron and the nuclear spin of the nearby ^{13}carbon atom. The $|0\rangle-|2\rangle$ and $|2\rangle-|3\rangle$ transitions are driven, respectively, by MW and RF radiations, observing the selection rules.

II. ENTANGLEMENT GENERATION

To describe the N-V, we follow a model presented in detail in [10] and concentrate our discussions on the fine and hyperfine structure of the ground state of the N-V center coupled to the ^{13}C atom. When there is no external magnetic field aligned with the quantisation axis of the N-V center, the system has four spin levels in the ^{3}A manifold as depicted by Fig. 1. This is due to the degeneracy of the $m_s=\pm 1$ electronic spin ($S=1$) of the center and its interaction with the nuclear spin ($I=1/2$) of the carbon atom. For clarity and consistency, we adopt the same notations for the four spin states as those used in [10],

$$|0\rangle \equiv |0\rangle_e \otimes |0\rangle_n = \frac{1}{\sqrt{2}}(|\uparrow\downarrow\rangle + |\downarrow\uparrow\rangle)_e \otimes |\uparrow\rangle_n, \tag{1}$$

$$|1\rangle \equiv |0\rangle_e \otimes |1\rangle_n = \frac{1}{\sqrt{2}}(|\uparrow\downarrow\rangle + |\downarrow\uparrow\rangle)_e \otimes |\downarrow\rangle_n, \tag{2}$$

$$|2\rangle \equiv |1\rangle_e \otimes |0\rangle_n = \frac{1}{\sqrt{2}}(|\uparrow\uparrow\rangle + |\downarrow\downarrow\rangle)_e \otimes |\uparrow\rangle_n, \tag{3}$$

$$|3\rangle \equiv |1\rangle_e \otimes |1\rangle_n = \frac{1}{\sqrt{2}}(|\uparrow\uparrow\rangle + |\downarrow\downarrow\rangle)_e \otimes |\downarrow\rangle_n. \tag{4}$$

The states $\{|0\rangle_e, |1\rangle_e\}$ are eigenstates associated with the electronic spins $\{m_s=0,\ m_s=-1\}$, while the states $\{|\uparrow\rangle_n, |\downarrow\rangle_n\}$ correspond to the nuclear spins $\{m_I=-1/2,\ m_I=+1/2\}$. From [10], the $|0\rangle-|2\rangle$ and $|2\rangle-|3\rangle$ transitions are found to be $\omega_{02}\approx 2.88$ GHz and $\omega_{03}\approx 130$ MHz, respectively, while $\omega_{01}\approx 2$ MHz. In general, the two frequencies ω_m and ω_r can be set slightly off resonance by the respective detunings δ_m and δ_r. We further assume that these detunings have unknown but constant values in the case of off-resonance errors.

The Hamiltonian of the system described in Fig. 1 can be expressed as

$$\hat{H} = \omega_{02}\hat{\sigma}_{22} + \omega_{03}\hat{\sigma}_{33} + \omega_{01}\hat{\sigma}_{11} - \frac{1}{2}(\Omega_m e^{i\omega_m t}\hat{\sigma}_{20} + \Omega_r e^{i\omega_r t}\hat{\sigma}_{23} + \text{H.c.}), \tag{5}$$

where $\hat{\sigma}_{pq}=|p\rangle\langle q|$ and $\Omega_m(\Omega_r)$ are the MW (RF) Rabi frequencies driving the electron-spin-resonance (ESR) and NMR transitions, respectively. The first line of Eq. (5) is the self-energy of the system relative to the ground state $|0\rangle$, while the reminder of the Hamiltonian describes the interaction of the external radiation with the system.

In the interaction picture, we have the effective Hamiltonian

$$\hat{H}_{eff} = \frac{1}{3}\delta(\hat{\sigma}_z^{20} + \hat{\sigma}_z^{23}) - \frac{1}{2}u_m(\cos\,\theta_m\hat{\sigma}_x^{20} + \sin\,\theta_m\hat{\sigma}_y^{20}) - \frac{1}{2}u_r(\cos\,\theta_r\hat{\sigma}_x^{23} + \sin\,\theta_r\hat{\sigma}_y^{23}), \tag{6}$$

where $\Omega_{m,r}=u_{m,r}\exp(i\theta_{m,r})$, $\hat{\sigma}_x^{pq}=\hat{\sigma}_{pq}+\hat{\sigma}_{qp}$, and $\hat{\sigma}_y^{pq}=i(\hat{\sigma}_{pq}-\hat{\sigma}_{qp})$. For simplicity, the detunings are assumed to be the same, i.e., $\delta_m=\delta_r=\delta$. We note that $u_{m,r}$ and $\theta_{m,r}$ are real, and they describe the control amplitudes and control phases.

We can clearly see from Eq. (6) that the Hamiltonian of the system is reduced effectively from the four-state system to a three-state system involving only the states $|0\rangle$, $|2\rangle$, and $|3\rangle$, which can simply be expressed in a matrix form as

$$\hat{H}_{eff} = -\frac{1}{2}\begin{pmatrix} \frac{2}{3}\delta & u_m e^{-i\theta_m} & 0 \\ u_m e^{i\theta_m} & -\frac{4}{3}\delta & u_r e^{i\theta_r} \\ 0 & u_r e^{-i\theta_r} & \frac{2}{3}\delta \end{pmatrix}. \tag{7}$$

We now consider the sequential application of MW and RF unitaries, $\hat{U}_r$ and $\hat{U}_m$, via rectangular control pulses to generate the state

$$|\psi_B\rangle = \hat{U}_r\hat{U}_m|0\rangle = \frac{1}{\sqrt{2}}(|0\rangle - |3\rangle) = \frac{1}{\sqrt{2}}(|0,0\rangle - |1,1\rangle). \tag{8}$$

Considering the resonant case, i.e., $\delta=0$, we first apply a microwave pulse on the $|0\rangle\leftrightarrow|2\rangle$ transition for time $t_m=\frac{\pi}{2}u_m^{-1}$, to get $\hat{U}_m=\exp(-i\hat{H}_{eff}t_m)=\exp(\frac{1}{4}i\hat{\sigma}_y^{20})$, giving the state $|\psi_M\rangle=\hat{U}_m|0\rangle=\frac{1}{\sqrt{2}}(|0\rangle-|2\rangle)$. Switching off the microwave radiation and subsequently applying a radio-frequency pulse with a phase of $\theta_r=\frac{\pi}{2}$, for a duration of $t_r=\pi u_r^{-1}$, on resonance with the $|2\rangle\leftrightarrow|3\rangle$ transition, produces the gate $\hat{U}_r=\exp(-i\hat{H}_{eff}t_r)=\exp(\frac{\pi}{2}i\hat{\sigma}_y^{23})$, which transforms the state $|\psi_M\rangle$ into the intended state $|\psi_B\rangle$.

The state $|\psi_B\rangle$ is an entangled Bell state in the coupled system of electronic and nuclear spins. In a brief summary, the sequential application above generates a sequential unitary gate $\hat{U}_{sq}$,

$$\hat{U}_{sq} = \hat{U}_r \hat{U}_m = \frac{1}{\sqrt{2}} \begin{pmatrix} 1 & 1 & 0 \\ 0 & 0 & -\sqrt{2} \\ -1 & 1 & 0 \end{pmatrix}, \tag{9}$$

which takes a total time $t_{sq} = t_m + t_r = \frac{3\pi}{2} u_m^{-1}$, if the amplitudes $u_m = u_r$. We expect that the gate implementation time can be shortened by a simultaneous irradiation of both the MW and RF transitions but the specific pulse sequence required cannot be easily derived analytically. In what follows we find that GRAPE derived robust pulses involving simultaneous irradiation are significantly shorter that their sequential composite pulse counterparts.

III. SYSTEMATIC ERRORS

To study the effects of systematic errors on the gate fidelity, we first quantify the PLE and ORE by two error fractions $\epsilon_f = (T' - T)/T$ and $\epsilon_g = \delta/\Lambda$, respectively, where $-1 \leq \{\epsilon_f, \epsilon_g\} \leq 1$. We use T and T' to denote the ideal and nonideal pulse application duration times and Λ is taken to be the fixed maximum amplitude of the microwave or radio-frequency pulses. In the presence of off-resonance error we consider the case when in the sequential pulse, $\max\{u_m\} = \max\{u_r\} = \Lambda$.

When the sequential pulse suffering from pulse-length error is applied to the system, the actual gate executed is highly dependent on the error fraction ϵ_f, and we can write

$$\hat{U}^f_{sq} = \hat{U}^f_r \hat{U}^f_m = \exp[\pi/2(1+\epsilon_f) i \hat{\sigma}^{23}_y] \exp[\pi/4(1+\epsilon_f) i \hat{\sigma}^{20}_y]. \tag{10}$$

We use the standard gate overlap fidelity F to measure the closeness between the generated gate, say $\hat{U}_a$, and the target gate $\hat{U}_i$ [14], we have

$$F = \left| \frac{\mathrm{Tr}(\hat{U}^\dagger_a \hat{U}_i)}{\mathrm{Tr}(\hat{U}^\dagger_i \hat{U}_i)} \right|^{1/2}. \tag{11}$$

One can show that the fidelity of the actual gate $\hat{U}^f_{sq}$ with respect to the ideal one $\hat{U}_{sq}$ is

$$F^f_{sq} \approx 1 - \frac{5\pi^2}{96} \epsilon_f^2 + \frac{\pi^4}{4608} \epsilon_f^4, \tag{12}$$

and we numerically plot this as Line 1 in Fig. 2. The quadratic term, ϵ_f^2, in Eq. (12) significantly reduces the fidelity. Hence, it is very desirable to find other types of control pulse that can suppress and possibly eliminate this quadratic dependence in the gate fidelity.

In the presence of the off-resonance error, the actual gate implemented by the sequential pulse is

$$\hat{U}^g_{sq}(\epsilon_g) = \hat{U}^g_r(\epsilon_g) \hat{U}^g_m(\epsilon_g), \tag{13}$$

where

$$\hat{U}^g_r = \exp\left[-\frac{\pi}{3} i \epsilon_g (\hat{\sigma}^{20}_z + \hat{\sigma}^{23}_z) + \frac{\pi}{2} i \hat{\sigma}^{23}_y \right], \tag{14}$$

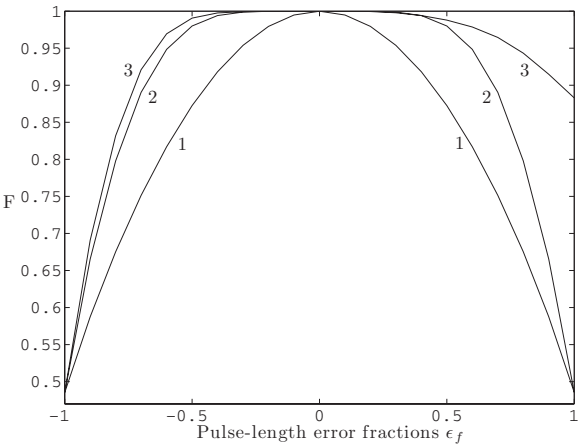

FIG. 2. Robust pulse control in the case of pulse-length error: Fidelity plots for the sequential pulse (Line 1), the BB1 composite pulse (Line 2), and the GRAPE pulse (Line 3) against PLE. We find that the GRAPE pulse achieves a greater level of fidelity over a larger range of PLE error, i.e., it is more robust that the other two control methods.

$$\hat{U}^g_m = \exp\left[-\frac{\pi}{6} i \epsilon_g (\hat{\sigma}^{20}_z + \hat{\sigma}^{23}_z) + \frac{\pi}{4} i \hat{\sigma}^{20}_y \right]. \tag{15}$$

Due to the complexity of the analytical expressions, the fidelity of the gate $\hat{U}^g_{sq}$ is calculated numerically and plotted as Line 1 in Fig. 3.

A. Composite pulses

Originally invented in NMR by Levitt and Freeman [15], composite pulses offset the effect of systematic errors by replacing single-quantum operations with several quantum operations which are designed to cancel out systematic errors. Composite pulses have been developed to implement robust arbitrary single qubit gate operations [13,16]. In our case, we apply two particular types of composite pulses, (A)

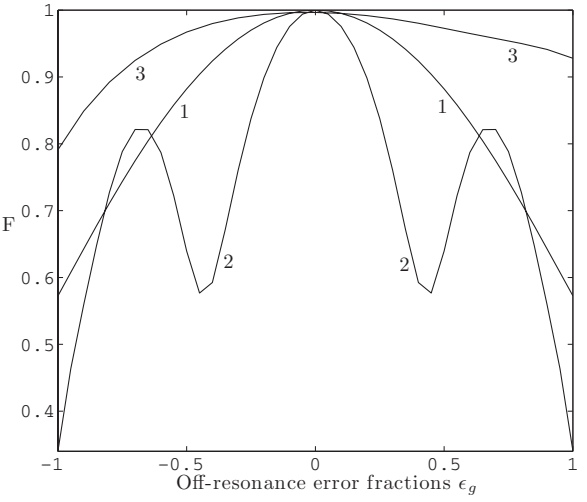

FIG. 3. Robust pulse control in the case of off-resonance error: Fidelity plots for the sequential pulse (Line 1), the CORPSE composite pulse (Line 2), and the GRAPE pulse (Line 3) against ORE.

broad band number 1 (known as BB1) composite pulses to correct for PLEs and (B) compensation for off-resonance errors, with a pulse sequence (known as CORPSE) to correct for OREs.

To apply these composite pulses, we first define generalized forms of the pulses subject to imperfect microwave and radio-frequency controls. In the presence of pulse-length error, these generalized forms are

$$\hat{\mathcal{U}}_m^f(\tau_m,\theta_m)=\exp\left[i\frac{1}{2}(\cos\ \theta_m\hat{\sigma}_x^{20}+\sin\ \theta_m\hat{\sigma}_y^{20})u_m(1-\epsilon_f)\tau_m\right], \tag{16}$$

$$\hat{\mathcal{U}}_r^f(\tau_r,\theta_r)=\exp\left[i\frac{1}{2}(\cos\ \theta_r\hat{\sigma}_x^{23}+\sin\ \theta_r\hat{\sigma}_y^{23})u_r(1-\epsilon_f)\tau_r\right]. \tag{17}$$

On the other hand, the generalized quantum operations in the case of off-resonance errors are

$$\hat{\mathcal{U}}_m^g(\tau_m,\theta_m)=e\left\{-i\left[\frac{i\epsilon_g}{3}\hat{Z}-\frac{1}{2}(\cos\ \theta_m\hat{\sigma}_x^{20}+\sin\ \theta_m\hat{\sigma}_y^{20})\right]u_m\tau_m\right\}, \tag{18}$$

$$\hat{\mathcal{U}}_r^g(\tau_r,\theta_r)=\exp\left\{-i\left[\frac{i\epsilon_g}{3}\hat{Z}-\frac{1}{2}(\cos\ \theta_m\hat{\sigma}_x^{23}+\sin\ \theta_m\hat{\sigma}_y^{23})\right]u_r\tau_r\right\}, \tag{19}$$

where $\hat{Z}=\hat{\sigma}_z^{20}+\hat{\sigma}_z^{23}$.

We consider the composite pulse analog of the sequential gate (10) to be obtained by replacing $\hat{U}_m^f$ and $\hat{U}_r^f$ with their composite pulse counterparts. For pulse-length errors we use BB1 composite pulses to replace U_m^f and U_r^f by $\hat{\mathcal{C}}_m^f$ and $\hat{\mathcal{C}}_r^f$ [13],

$$\hat{\mathcal{C}}_m^f=\hat{\mathcal{U}}_m^f\left(\frac{\pi}{4},\frac{\pi}{2}\right)\hat{\mathcal{U}}_m^f(\pi,1.04\pi)\times\hat{\mathcal{U}}_m^f(2\pi,2.12\pi)\hat{\mathcal{U}}_m^f(\pi,1.04\pi)\hat{\mathcal{U}}_m^f\left(\frac{\pi}{4},\frac{\pi}{2}\right), \tag{20}$$

$$\hat{\mathcal{C}}_r^f=\hat{\mathcal{U}}_r^f\left(\frac{\pi}{2},\frac{\pi}{2}\right)\hat{\mathcal{U}}_r^f(\pi,1.08\pi)\times\hat{\mathcal{U}}_r^f(2\pi,2.24\pi)\hat{\mathcal{U}}_r^f(\pi,1.08\pi)\hat{\mathcal{U}}_r^f\left(\frac{\pi}{2},\frac{\pi}{2}\right), \tag{21}$$

where τ_m and τ_r are expressed in the units of u_m^{-1} and u_r^{-1}. One can verify that in the absence of PLE, we have $\hat{\mathcal{C}}_r^f(\epsilon_f=0)\hat{\mathcal{C}}_m^f(\epsilon_f=0)=\hat{U}_{sq}$. The composite pulses $\hat{\mathcal{C}}^f=\hat{\mathcal{C}}_r^f\hat{\mathcal{C}}_m^f$ take a total time $\tau^f=9\frac{1}{2}\pi u_m^{-1}$ when both real amplitudes $u_m=u_r$ are identical. The total time is roughly 6.33 times longer than that of the sequential pulse. The fidelity of the BB1 composite gate, $\hat{\mathcal{C}}^f$, is plotted as Line 2 in Fig. 2, and is numerically calculated through the following equation:

$$F_c^f=\left|\frac{\mathrm{Tr}(\hat{\mathcal{C}}^{f\dagger}\hat{U}_{sq})}{\mathrm{Tr}(\hat{U}_{sq}^{\dagger}\hat{U}_{sq})}\right|^{1/2}. \tag{22}$$

From Fig. 2 we see that the range of fidelity $F\geq 0.9$ has expanded. In contrast with the sequential gate, where the fidelity $F\geq 0.9$ holds approximately only for $|\epsilon_f|<0.4$, the BB1 composite gate maintains this level of fidelity for $|\epsilon_f|<0.7$.

In the case of ORE, we replace the gates $\hat{U}_m^g$ and $\hat{U}_r^g$ with their CORPSE counterparts [16],

$$\hat{\mathcal{C}}_m^g=\hat{\mathcal{U}}_m^g\left(2.14\pi,\frac{\pi}{2}\right)\hat{\mathcal{U}}_m^g\left(1.77\pi,-\frac{\pi}{2}\right)\hat{\mathcal{U}}_m^g\left(0.14\pi,\frac{\pi}{2}\right), \tag{23}$$

$$\hat{\mathcal{C}}_r^g=\hat{\mathcal{U}}_r^g\left(7\pi/3,\frac{\pi}{2}\right)\hat{\mathcal{U}}_r^g\left(5\pi/3,-\frac{\pi}{2}\right)\hat{\mathcal{U}}_r^g\left(\pi/3,\frac{\pi}{2}\right), \tag{24}$$

to produce the complete gate $\hat{\mathcal{C}}^g=\hat{\mathcal{C}}_r^g\hat{\mathcal{C}}_m^g$, which takes a total time of $\tau^g\approx 5.59\times t_{sq}$. This is nearly six times longer than the sequential pulse, assuming $u_m=u_r$. We plot the fidelity of the gate numerically calculated based on Eq. (11) as Line 2 in Fig. 3, and find that the CORPSE pulse performs very poorly in correcting the off-resonance error. This is due to the Autler-Townes splitting of the NMR transition due to the ESR excitation of the MW transition [17]. Thus one cannot use the standard CORPSE pulse in each of the ESR and NMR sequential pulses to correct for ORE.

B. Robust GRAPE pulses

We now explore whether one can obtain robust operations in a shorter time than the composite pulses by simultaneous irradiation both the MW and RF transitions. Rapid and robust control quantum control is important as the total gate duration significantly determines the number of quantum operations that can be performed before decoherence degrades the quantum coherence. Initially proposed for NMR experiments, the GRAPE algorithm produce pulses that minimize the time required to implement a target unitary operator [12] and some quantum algorithmic elements [14]. GRAPE pulses have been experimentally demonstrated in a single qubit trapped ion system [18]. A GRAPE based scheme is also proposed to control a coupled Josephson qubit system [19], and later was extended to control open quantum systems in the Markovian domain [20]. It has also been applied in implementing high-fidelity single qubit operations in a noisy environment due to random telegraph noise in superconducting solid-state qubits [21].

We briefly summarize how the GRAPE algorithm works [12] and how it can achieve time-optimal control and robustness against systematic errors. We start by writing the unitary evolution under the Hamiltonian (6) in the form of

$$\hat{U} = \mathcal{T}\int \exp\left\{-i\left[\hat{H}_s + \sum_{k=1}^{4} u_k(t)\hat{H}_k\right]t\right\}dt, \tag{25}$$

where $u_k(t)$ and $\hat{H}_k$ are the control pulses and control Hamiltonians, expressed as follows:

$$u_{1,3}(t) = -\frac{1}{2}u_{m,r}(t)\cos\,\theta_{m,r}(t),$$

$$u_{2,4}(t) = -\frac{1}{2}u_{m,r}(t)\sin\,\theta_{m,r}(t), \tag{26}$$

and $\{\hat{H}_1,\hat{H}_2,\hat{H}_3,\hat{H}_4\}=\{\hat{\sigma}_x^{20},\hat{\sigma}_y^{20},\hat{\sigma}_x^{23},\hat{\sigma}_y^{23}\}$, and $\hat{H}_s$ is a drift Hamiltonian, $\hat{H}_s=\frac{1}{3}\delta(\hat{\sigma}_z^{20}+\hat{\sigma}_z^{23})=\frac{1}{3}\delta\hat{Z}$, and with the initial condition, $\hat{U}(t=0)=\hat{I}$. We wish to numerically optimize the controls $u_k(t)$, in a particular application time $t=T$, such that $\hat{U}(T)$ approaches a target gate $\hat{U}_T$. This is equivalent to maximizing a performance function P,

$$P = |\mathrm{Tr}\,\hat{U}_T^{\dagger}\hat{U}(T)|^2. \tag{27}$$

One considers discretizing time $\Delta t=T/N$, where N is a number of time steps/bins, and during each time bin the control u_k's are constant. We can approximate Eq. (25),

$$\hat{U} = \hat{U}_N\hat{U}_{N-1}\cdots\hat{U}_1, \tag{28}$$

which gives the performance function approximately to be

$$P = \mathrm{Tr}(\hat{U}_T^{\dagger}\hat{U}_N\hat{U}_{N-1}\ldots\hat{U}_1)\times\mathrm{Tr}[(\hat{U}_1\ldots\hat{U}_{N-1}\hat{U}_N)^{\dagger}\hat{U}_T]. \tag{29}$$

From [12], the gradient $g(j)=\delta P/\delta u_k(j)$ to $O(\Delta t)$ is written as

$$g(j) = -2\,\mathrm{Re}(\mathrm{Tr}(i\Delta t\hat{A}_j^{\dagger}\hat{H}_k\hat{B}_j)\mathrm{Tr}(\hat{B}_j^{\dagger}\hat{A}_j)), \tag{30}$$

where $\hat{A}_j=\hat{U}_{j+1}^{\dagger}\ldots\hat{U}_N^{\dagger}\hat{U}_T$ and $\hat{B}_j=\hat{U}_j\ldots\hat{U}_1$, and the performance function P always increases if we update

$$u_k(j)\rightarrow u_k(j)+\epsilon g(j), \tag{31}$$

where a small step size ϵ is used. It is also necessary to add an additional term $g_{\max}(j)$,

$$g_{\max}(j) = -2\alpha_p u_k(j)\Delta t, \tag{32}$$

to the gradient $g(j)$, to penalize excessive microwave or radio-frequency power.

The pulse-length and off-resonance errors are incorporated into the algorithm by replacing the ideal $\hat{U}_j$, in Eq. (28) with $\hat{U}_j^f$ and $\hat{U}_j^g$ written as

$$\hat{U}_j^{\epsilon_f} = \exp\left\{-i\Delta t(1-\epsilon_f)\left[\sum_{k=1}^{4} u_k(j)\hat{H}_k\right]\right\}, \tag{33}$$

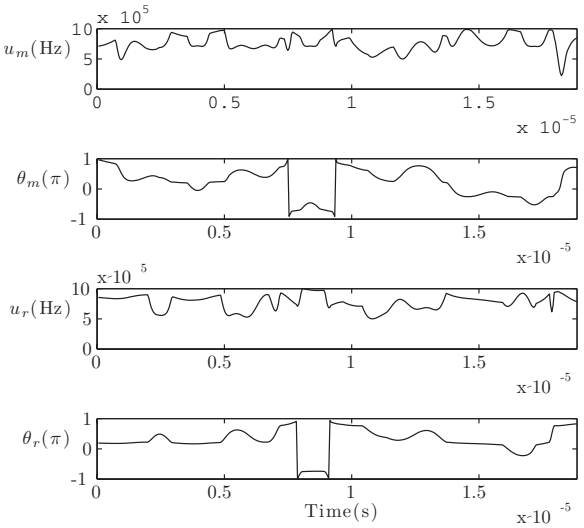

FIG. 4. The real amplitudes and phases of the microwave and radio-frequency pulses engineered by the GRAPE algorithm to create an entangling gate which is the robust against the pulse-length errors (PLE). The application time is $6\pi\mu s$ and the maximum real amplitude is 1 MHz.

$$\hat{U}_j^{\epsilon_g} = \exp\left\{-i\Delta t\left[\epsilon_g\hat{H}_s + \sum_{k=1}^{4} u_k(j)\hat{H}_k\right]\right\}. \tag{34}$$

The performance function to be optimized is the average performance function over set of error fractions, and defined as

$$P^{f,g} = \frac{1}{N(\vec{\epsilon}_{f,g})}\sum_{\min\{\vec{\epsilon}_{f,g}\}}^{\max\{\vec{\epsilon}_{f,g}\}}\mathrm{Tr}(\hat{U}_T^{\dagger}\hat{U}_N^{\epsilon_{f,g}}\hat{U}_{N-1}^{\epsilon_{f,g}}\ldots\hat{U}_1^{\epsilon_{f,g}}) \times\mathrm{Tr}((\hat{U}_1^{\epsilon_{f,g}}\ldots\hat{U}_{N-1}^{\epsilon_{f,g}}\hat{U}_N^{\epsilon_{f,g}})^{\dagger}\hat{U}_T), \tag{35}$$

for the case of PLE or ORE (denoted by superscripts f or g), where $N(\vec{\epsilon}_{f,g})$ is a number of elements in the set of error fractions $\vec{\epsilon}_{f,g}$ we wish to optimize over. This modification allows us to optimize the control pulses u_k, only over a certain range of error fractions, for example $-0.2\leq\epsilon_{f,g}\leq 0.2$. However, the real performance of the optimized pulse is checked through the gate fidelity as defined by Eq. (11).

IV. DISCUSSION ON NUMERICAL SIMULATIONS

In our numerical simulations, the modified GRAPE algorithms explained in the previous section are executed using MATLAB to produce a set of optimized microwave and radio-frequency pulses presented in Figs. 4 and 5. Both sets of pulses have $N=400$ and $\max\{u_m\}=\max\{u_r\}=1$ MHz and this limit is realistic in current N-V ESR/NMR ODMR experiments. We found that by simultaneous irradiation we are able to reduce the time taken to achieve robust operation with respect to both the pulse-length and off-resonance errors. In the case of PLE, the GRAPE pulse time is four times longer than that of the sequential pulse, i.e., approximately 37% faster than the BB1 composite pulse time. The GRAPE pulse takes only around 36% of the CORPSE pulse time, in the

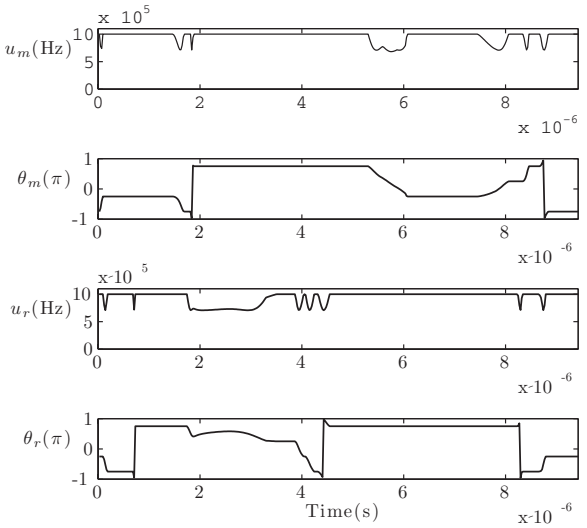

FIG. 5. The real amplitude and phases of microwave and radio-frequency pulses engineered by the GRAPE algorithm to create an entangling gate which is the robust against off-resonance errors (ORE). The application time and the maximum real amplitude are the same as those in the case of PLE.

case of off-resonance error. In engineering the GRAPE pulses, we manually re-optimize the pulses by adjusting the range of the error fractions and the duration several times until the gate reaches a considerably high fidelity.

In both cases of pulse-length and off-resonance errors, the gate fidelity of the optimized pulses via GRAPE outperforms those of the sequential pulses and the composite pulses for every value of the PLE and ORE fractions, as shown by Line 3 in Figs. 2 and 3. However, the BB1 composite pulse does better than the sequential pulse in the case of pulse-length error. It is interesting to note that the CORPSE composite pulse, which is robust against ORE in a single two-level system, is no longer robust against the ORE in our essentially three-level system. Hence, further investigations would be needed in order to develop composite pulses that can tackle the off-resonance error in a three-level system. This is beyond the scope of this paper. There are puzzling asymmetries in the fidelity plots of the GRAPE pulses in both the cases of ORE and PLE (Line 3 in Figs. 2 and 3). These asymmetries can also be found in the earlier literature [18]. In the pulse-length error case, we suspect these asymmetries may be due to the increased available power within the pulse for $\epsilon_f > 0$.

TABLE I. Performance comparisons between the CORPSE and GRAPE pulses for different detunings and maximum Rabi frequencies in the case of off-resonance error. The parameters used in the simulations are $N=400$ and $\max\{u_m\}=1$ MHz.

c_λ	$\max\{u_r\}$ (MHz)	τ_C	τ_G	κ_C	κ_G
0.8	1	5.59	2	0.3242	1.5379
1.2	1	5.59	2	0.3215	1.9400
1.4	1	5.59	2	0.2618	1.7982
1.2	0.5	5.07	3.5	0.3422	1.1793

TABLE II. Performance comparisons between the BB1 and GRAPE pulses for two different maximum RF Rabi frequencies in the presence of pulse-length error. We use the same numerical parameters, $N=400$ and $\max\{u_m\}=1$ MHz in the simulations.

$\max\{u_r\}$ (MHz)	τ_B	τ_G	κ_B	κ_G
0.5	5.8	3.5	1.5119	1.8588
0.25	5.4	3	1.5119	1.744

To expand on the analysis above, we can relax the constraints of identical detuning parameters and maximum Rabi frequencies in the microwave and radio-frequency control pulses, i.e., $\delta_m \neq \delta_r$ and $\max\{u_m\} \neq \max\{u_r\}$. We consider the more general case of ORE where the detuning parameters are correlated by a constant factor $c_\lambda = \delta_m / \delta_r$, and simulate this condition for a few values of c_λ, to obtain the robust GRAPE pulses. The performances of the numerically optimized pulses and their comparisons with the sequential and the CORPSE pulses are found to be similar to those depicted in Fig. 3. To avoid the redundancy of fidelity plots and pulse sequences, we define two performance quantities: $\tau_{\{C,B,G\}}$ and $\kappa_{\{C,B,G\}}$, where a set of subscripts $\{C,B,G\}$ denotes the {CORPSE,BB1,GRAPE} pulses. The first quantity, $\tau_{\{C,B,G\}}$, is the CORPSE/BB1/GRAPE pulse time duration divided by the corresponding sequential pulse time. Meanwhile, the second quantity is the width of the error fractions of the CORPSE/BB1/GRAPE pulse that have $F \geq 0.95$, divided by that of the sequential pulse. Ideally, we would like τ as small as possible while κ as large as possible. We present these quantities for four combinations of different c_λ and $\max\{u_r\}$ in Table I, and find that the GRAPE pulses are still faster and more robust than the CORPSE pulse. In the case of pulse-length error, we simulate the two conditions of $\max\{u_m\} \neq \max\{u_r\}$, as presented in Table II, and find that the GRAPE pulses again outperform the BB1 composite pulse.

While the maximum real amplitudes of the optimized pulses used in our analyses are not technologically difficult to implement [8,9,11], the fast controlling apparatuses required to rapidly change the pulse amplitudes and phases is quite demanding since they should be able to operate on nanosecond time scales.

V. CONCLUSION

We have numerically optimized the microwave and radio-frequency pulses required to create the entanglement in the system of single N-V center coupled to the nearest carbon atom through the modified GRAPE algorithm. We have found that the entangling gate created by such optimized pulses is more robust against systematic errors and has faster implementation time than that required by the corresponding composite pulses. Reasonable extensions of our work would be considering the simultaneous presence of PLE and ORE in the system and taking into account decoherence processes. For the latter one will need to model an open quantum system through a master equation.

ACKNOWLEDGMENTS

We highly acknowledge the referees for their constructive comments and suggestions, and gratefully thank T. Gaebel, J. Beck, F. Jelezko, and S. Rebic for helpful discussions. This work was partially supported under the European Commission FP6 IST FET QIPC project QAP under Contract No. 015848.

[1] B. E. Kane, Fortschr. Phys. **48**, 1023 (2000).
[2] J. J. L. Morton, A. M. Tyryshkin, R. M. Brown, S. Shankar, B. W. Lovett, A. Ardavan, T. Schenkel, E. E. Haller, J. W. Ager, and S. A. Lyon, Nature (London) **455**, 1085 (2008).
[3] M. Kroutvar, Y. Ducommun, D. Heiss, M. Bichler, D. Schuh, G. Abstreiter, and J. J. Finley, Nature (London) **432**, 81 (2004).
[4] Y. Nakamura, Yu. A. Pashkin, and J. S. Tsai, Nature (London) **398**, 786 (1999).
[5] R. J. Schoelkopf and S. M. Girvin, Nature (London) **451**, 664 (2008).
[6] M. V. Gurudev Dutt, L. Childress, L. Jiang, E. Togan, J. Maze, F. Jelezko, A. S. Zibrov, P. R. Hemmer, and M. D. Lukin, Science **316**, 1312 (2007).
[7] F. Jelezko and J. Wrachtrup, J. Phys.: Condens. Matter **16**, R1089 (2004).
[8] F. Jelezko, T. Gaebel, I. Popa, A. Gruber, and J. Wrachtrup, Phys. Rev. Lett. **92**, 076401 (2004).
[9] F. Jelezko, T. Gaebel, I. Popa, M. Domhan, A. Gruber, and J. Wrachtrup, Phys. Rev. Lett. **93**, 130501 (2004).
[10] A. P. Nizovtsev, S. Ya. Kilin, F. Jelezko, T. Gaebal, I. Popa, A. Gruber, and J. Wrachtrup, Opt. Spectrosc. **99**, 233 (2005).
[11] P. Neumann, N. Mizuochi, F. Rempp, P. Hemmer, H. Watanabe, S. Yamasaki, V. Jacques, T. Gaebel, F. Jelezko, and J. Wrachtrup, Science **320**, 1326 (2008).
[12] N. Khaneja, T. Reiss, C. Kehlet, T. Schulte-Herbrüggen, and S. J. Glaser, J. Magn. Reson. **172**, 296 (2005).
[13] H. K. Cummins, G. Llewellyn, and J. A. Jones, Phys. Rev. A **67**, 042308 (2003).
[14] T. Schulte-Herbrüggen, A. Spörl, N. Khaneja, and S. J. Glaser, Phys. Rev. A **72**, 042331 (2005).
[15] M. H. Levitt and R. Freeman, J. Magn. Reson. **33**, 473 (1979).
[16] H. K. Cummins and J. A. Jones, New. J. Phys. **2**, 6 (2000).
[17] C. Wei and N. B. Manson, Phys. Rev. A **60**, 2540 (1999).
[18] N. Timoney, V. Elman, S. Glaser, C. Weiss, M. Johanning, W. Neuhauser, and Chr. Wunderlich, Phys. Rev. A **77** 052334 (2008).
[19] A. Spörl, T. Schulte-Herbrüggen, S. J. Glaser, V. Bergholm, M. J. Storcz, J. Ferber, and F. K. Wilhelm, Phys. Rev. A **75**, 012302 (2007).
[20] T. Schulte-Herbrüggen, A. Spörl, N. Khaneja, and S. Glaser, e-print arXiv:quant-ph/0609037.
[21] M. Möttönen, R. de Sousa, J. Zhang, and K. B. Whaley, Phys. Rev. A **73**, 022332 (2006).